Extended Traveling Wave Theory for the Multi-stage Tower under a Direct Lightning Strike

Yuxuan Ding[1], Binghao Li[1], Y. Du[1], Mingli Chen[1], Zhe Li[2] and and Yu-ming Zhao[2]
[1]The Hong Kong Polytechnic University , Dept.of Building Services Engineering, Hong Kong, China
[2]China Southern Power Grid Company limited, Shenzhen Power Supply Bureau, Shenzhen, China

Abstract— **This paper presents a theoretical time-domain analysis of lightning surge propagation on a multi-stage and multi-conductor tower. An extended traveling wave theory using electric scalar potential is introduced. The non-TEM wave propagation in the tower is characterized by time/positon-variant transient impedance. The analytical formulas of the transient impedance are presented for any position/time in the tower, as well as those of the reflection coefficient at a discontinuity. The concept of primary and secondary waves is introduced to depict the multiple reflections in the tower. It is found that the primary current wave attenuates during its propagation in the tower, and is corrected by a factor when crossing over the discontinuity. A pair of secondary waves are generated at the discontinuity, similar to a center-fed dipole. The proposed method is applied to evaluate the lightning current in a two-stage tower. The result of the proposed method is of high consistency with the FDTD result. It is also observed that the secondary waves could be neglected if the reflection coefficient is small. The traditional transmission line theory could lead to a significant error of the current in the tower.**

Keywords- lightning, tower, transmission line, dipole

I. INTRODUCTION

Transmission towers are of great significance in lightning research, as they are the essential part in the analysis of lightning surges on overhead power lines [1]-[3]. Inappropriate tower modeling may fail to predict the flashover rate [4], and lead to incorrect assessment of hazards to sensitive loads. On the other hand, the resultant current propagating on a tower could be a significant source in the evaluation of lightning-induced electromagnetic pulses (LEMP) [5]-[6]. The correct current distribution along a tower, therefore, is indispensable in lightning transient analysis.

Research work has been carried out extensively to reveal the lightning current in the tower using lumped representations. Several models has been proposed, including the single-line model [4], [7-9], multi-conductor model [10]-[12], multi-story model [13]-[14]. The simplest representation probably is the one with constant surge impedance and travel time based on the transmission line (TL) theory [4]. Note that, the TL theory introduces forward and backward waves along a line as well as the reflection at the boundary, which is of great convenience in its application. Nevertheless, the TL theory is based on the TEM-mode assumption and both the impedance and reflection coefficients are constant. This is not in incoincidence with the observation results of lightning surges along vertical structures. Several expressions of time-variant surge impedance at the tower tip have been proposed [33-34]. For example, authors in [34] proposed the method for computing the time-variant surge impedance for a transmission tower by using the vector potential. However, the current is assumed uniform along the tower, this is still a TL theory approximation. Other authors give both the theoretical and experimental studies on the reflection coefficient at the tower tip and tower base [17]. It is found that the reflection coefficient in a tower is time-variant and dependent on the current waveform. However, the analysis method is again based on the TL theory.

In [18] the phenomenon of non-TEM wave propagation in a vertical conductor has been reported. Unlike the TEM wave, this wave is described using the electric scalar potential and current in the vertical structure, because the definition of quasi-static transverse voltage does not guarantee a unique value of the voltage on the tower [19]. It also is found that both the surge impedance [20] and corresponding current attenuation [21]-[22] are time/position-variant. These studies, however, could not fully explain and formulate the varying surge impedance of a non-TEM wave [19]-[20]. The closed-form expression of the reflection coefficient and the dynamic behavior of a non-TEM wave in the tower with a discontinuity remain unknown. Meanwhile, the well known Bewley traveling-wave lattice diagram [3] is used to describe the complicated multiple reflections in a multi-stage structure based on the TL theory. However, it cannot be directly applied for the non-TEM wave propagation.

It has been pointed out in [23]-[25] that theoretical studies are very useful in understanding the phenomena of transients in the tower. In this paper, a time-domain traveling wave theory is introduced for the transient analysis on a multi-stage and multi-conductor tower. This theory can be used to describe the propagation of a non-TEM wave along a multi-stage tower structure above the ground. In Section II, a generic configuration of the tower and its model are described. The wave propagation equations are presented in Section III for multiple lines in parallel, and in Section IV for the lines with a discontinuity. Closed-form formulas are provided for both the transient impedance and reflection coefficient. In Section V, a convolution technique is presented to determine the tower current under a source with an arbitrary waveform. Finally, the proposed theory is applied to evaluate lightning

transients in a two-stage tower on the ground. The comparison results using the FDTD method and the TL model are given in Section VI finally.

II. Multiple-Dipole Modle of a Tower Structure

Shown in Fig. 1(a) is a multi-stage tower subject to a lightning stroke at its top end. It is known that the lightning return stroke generates two current pulses propagating upwards in the channel, and downwards in the tower. These pulses may be viewed as the incident currents in the channel and tower resulting from a voltage source at the attachment point. With this model, the wave reflection at the channel base can then be fully taken into account during a lightning return stroke. This configuration is similar to a dipole fed by a delta-gap voltage source, as shown in Fig. 1. In this paper all the wires in the tower are assumed to be lossless, and the contribution of horizontal wires is neglected.

In the evaluation of lightning transients, a specific waveform is normally assigned to the incident current. In this paper, the incident current $I_{s,0}$ with a ramp waveform is considered first. The transients in the tower with an arbitrary current waveform are obtained by using a convolution technique presented in Section V.

It is known that a tower structure does not support TEM wave propagation [18-22]. Electric scalar potential ϕ together with current I then is used to describe the wave propagation in the tower. Note that the tower structure is rotationally symmetric, as seen in Fig. 1(a). All branch currents and scalar potentials are identical at the same height in a stage. The tower structure can then be represented by a set of identical dipole lines running in parallel. Each line has a feed current ($I_{s1,0}$) at $z = 0$ and a discontinuity between two stages. Fig. 1(b) shows the configuration of one representative dipole line, which is deformed at $z = 0$ and $z = z_0$. Note that $I_{s1,0} = I_{s,0}/n$ where n is the number of branches in the stage.

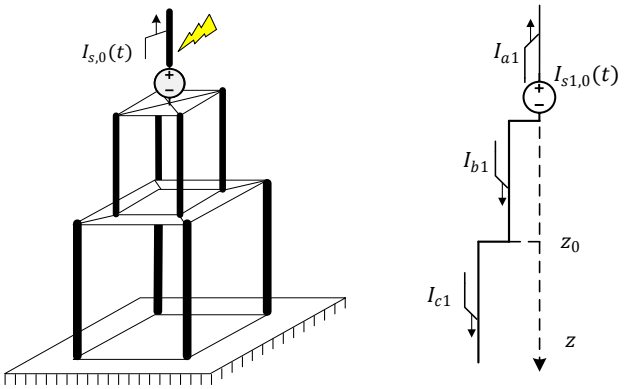

(a) Tower configuration (b) one dipole line

Fig. 1 Tower structure and its dipole line model

III. Wave Propagation on a Tower Model with Constant Wire Spacing

Consider a standalone center-fed dipole with two perfectly conducting thin wires, which is excited by a delta-gap voltage source. With a ramp incident current from the source, current I propagates with attenuation along the dipole, while scalar potential ϕ propagates without attenuation [26]. These parameters are uniquely determined by transient impedance Z of the dipole. Assume that the dipole wire has a radius of of r_x in one of its two arms or stage x. In stage x of a standalone dipole, they are described with the following characteristic equations,

$$\begin{aligned} \phi_x(z,t) &= \phi_x(0, t - z/c) \\ &= I_x(z,t) Z_x(z,t) \\ I_x(z,t) &= I_{s,0}(t - z/c)\alpha_x(z,t) \end{aligned} \tag{1}$$

where c is the speed of light, and α_x is the attenuation coefficient of current given by $Z_x(0, t - z/c)/Z_x(z,t)$. $I_{s,0}(t)$ is the ramp incident current at the feed point ($z = 0$). $Z_x(z,t)$ can be either evaluated numerically [26], or analytically [28] with (B6) in Appendix B.

Now consider a rotationally-symmetric model of n parallel dipole lines, which is fed separately by n voltage sources with the ramp current $I_{s,0}$ ($I_{s1,0} = I_{s,0}/n$) from the source. These dipole lines have a constant spacing of $D_{x,ij}$ between lines i and j, and a radius of r_x in stage x ($x = a$ or b). Fig, 2(a) illustrates the configuration of two dipole lines 1 and i of this model. In the model, the total stage current I_{xM} is equal to nI_{x1}, where I_{x1} is the current of one dipole line in stage x.

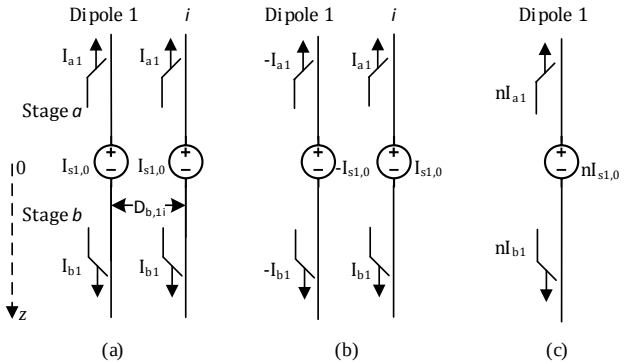

Fig.2 Multi-dipole model with constant wire spacing (a) original model, (b) one pair of dipole lines carrying balanced currents (c) single dipole line

It is known in Appendix A that electric potential ϕ_{xM} propagates without attenuation in the model. According to Appendix B, ϕ_{xM} and I_{xM}in this n-diploe line model can be expressed using tower transient impedance Z_{xM}, as follows:

$$\begin{aligned} \phi_{xM}(z,t) &= \phi_{xM}(0, t - z/c) \\ &= I_{xM}(z,t) Z_{xM}(z,t) \\ I_{xM}(z,t) &= I_{s,0}(t - z/c)\alpha_{xM}(z,t) \end{aligned} \tag{2}$$

where α_{xM} is the attenuation coefficient of current in the n-dipole line model. Both α_{xM} and Z_{xM} are given by

$$\begin{aligned} \alpha_{xM}(z,t) &= Z_{xM}(0, t - z/c)/Z_{xM}(z,t) \\ Z_{xM}(z,t) &= Z_x(z,t) - \frac{\mu_0 c}{2\pi n}\sum_{i=2}^{n} \ln(D_{x,1i}/r_x) \end{aligned} \tag{3}$$

$Z_x(z,t)$ is the transient impedance of a standalone dipole made of wire b. Note that both (1) and (3) are similar. An additional quasi-static transmission line impedance is added for this multi-dipole line structure.

IV. Wave Propagation over the Multi-dipole Line Model with a Discontinuity

A. Waves at the discontinuity of a dipole line model

Consider the *n*-dipole line model with a sudden change of wire spacing, as illustrated in Fig. 3(a). This dipole line model has the spacing of $D_{b,ij}$ in stage b, and $D_{c,ij}$ in stage c. The change of wire spacing is made at $z = z_0$.

Similar to the wave propagation in the standalone dipole with a discontinuity [27], incident current I^i_{bM} propagates in stage b towards the discontinuity. It then generates reflected current I^r_{bM} in stage b, and transmitted current $I^t_{cM} = I^{t1}_{cM} + I^{t2}_{cM}$ in stage c. These currents are combined into two groups: (1) I^r_{bM} and I^{t1}_{cM} and (2) I^i_{bM} and I^{t2}_{cM}. Fig. 3(b) and 3(c) show the configurations for these two sets of the currents. By ignoring the effect of short wires connecting stages b and c at $z = z_0$, the following boundary conditions are observed,

$$\begin{aligned} I^i_{bM}(z,t)\big|_{z=z_0} &= I^{t1}_{cM}(z,t)\big|_{z=z_0} \\ I^r_{bM}(\zeta,\tau)\big|_{\zeta=0} &= I^{t2}_{cM}(\zeta,\tau)\big|_{\zeta=0} \end{aligned} \tag{4}$$

where $\zeta = z - z_0$, $\tau = t - t_0$ and $t_0 = z_0/c$.

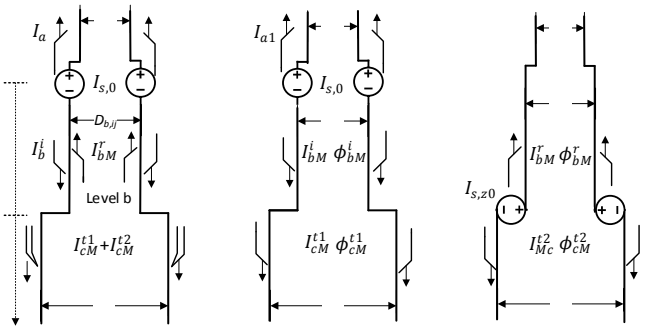

Fig. 3 Multi-dipole line model with a change of wire spacing (a) original model, (b) config. of I^r_{bM} and I^{t1}_{cM}, and (c) config. of I^i_{bM} and I^{t2}_{cM}.

In the configuration shown in Fig. 3(b), as indicated in Appendix C, both scalar potential $\phi^i_{bM}(z,t)$ and $\phi^{t1}_{cM}(z,t)$ are expressed respectively using corresponding branch currents I^i_{bM} and I^{t1}_{cM} in their stages, as follows:

$$\begin{aligned} \phi^i_{bM}(z,t) &= I^i_{bM}(z,t) Z_{bM}(z,t) \\ \phi^{t1}_{cM}(z,t) &= I^{t1}_{cM}(z,t) Z_{cM}(z,t) \end{aligned} \tag{5}$$

where $Z_{xM}(z,t)$ is the transient impedance of a multi-diploe line model, shown in Section III, with the same geometry as the wires in stage x. This indicates that both potential and current in a tower stage can be evaluated using a multi-diploe line model with constant spacing.

In Fig. 3(c), a set of voltage sources is inserted between stages b and c, the source current $I_{s,z0}(\tau)$ from the virtual source is equal to $I^r_{bM}(z_0,\tau)$ or $I^{t2}_{bM}(z_0,\tau)$, and is activated after the wave arrives at point z_0. This configuration is similar to the one shown in Section III. According to Appendix C, both backward and forward waves ϕ^r_{bM} and ϕ^{t2}_{cM} are expressed with transient impedance Z_{xM} as

$$\begin{aligned} \phi^r_{bM}(\zeta,\tau) &= -I_{s,z0}(\tau) Z_{bM}(\zeta,\tau) \\ \phi^{t2}_{cM}(\zeta,\tau) &= I_{s,z0}(\tau) Z_{cM}(\zeta,\tau) \end{aligned} \tag{6}$$

where both ζ and τ are respectively the position and time with respect to a local source at $z = z_0$. Note that $Z_{bM}(-\zeta,t)$ is evaluated with $Z_{bM}(\zeta,t)$ mathematically.

B. Reflection coefficient at the discontinuity

It is noteworthy that the potential at the discontinuity in this configuration is continuous, i.e., $\phi^i_{bM} + \phi^r_{bM} = \phi^{t1}_{cM} + \phi^{t2}_{cM}$ at $z = z_0$. With (5) and (6), the following equation for the reflection coefficient $\gamma_{z0}(\tau)$ is obtained,

$$\gamma_{z0}(\tau) = \frac{I_{sc}(\tau)}{I^i_{bM}(z_0, t - z_0/c)} = \frac{Z_{bM}(z_0,t) - Z_{cM}(z_0,t)}{Z_{bM}(0,\tau) + Z_{cM}(0,\tau)} \tag{7a}$$

Expression (7a) is similar to the reflection coefficient defined in the traditional traveling wave theory, in which the impedance is constant. With (C5) in Appendix C, the term of $Z_{bM} - Z_{cM}$ in (7a) can be further written as

$$Z_{bM}(z_0,t) - Z_{cM}(z_0,t) = \frac{\mu_0 c}{2\pi} \cdot \left[\ln\left(\frac{r_c}{r_b}\right) - \frac{1}{n}\sum_{i=2}^{n} \ln\left(\frac{r_c}{r_b} \cdot \frac{D_{b,1i}}{D_{c,1i}}\right) \right] \tag{7b}$$

Then the reflection coefficient in (7) is only determined by wire radius, wire spacing and input impedance at the point of discontinuity. This is in coincidence with the experiment reported in [17].

C. Traveling wave theory for the multi-dipole line model with a discontinuity

As seen in Appendix C, the propagation of scalar potentials in a set of perfectly conducting wires is lossless. It can then be stated that propagation of ϕ^r_{bM} and ϕ^{t2}_{cM} in Fig. 3(c) is lossless, as well as ϕ^i_{bM} and ϕ^{t1}_{cM} in Fig. 3(b). Therefore, both I^i_{bM} and I^{t1}_{cM} can be obtained with (5), and are expressed with the source current as

$$\begin{aligned} I^i_{bM}(z,t) &= I_{s,0}(t - z/c) \cdot \alpha_{bM}(z,t) \\ I^{t1}_{cM}(z,t) &= I^i_{bM}(z_0,t) / \alpha_{cM}(z_0,t) \cdot \alpha_{cM}(z,t) \end{aligned} \tag{8}$$

With (6) and $\alpha_x(-z,t) = \alpha_x(z,t)$ the following is obtained,

$$\begin{aligned} I^r_{bM}(\zeta,\tau) &= I_{s,z0}(\tau) \cdot \alpha_{bM}(\zeta,\tau) \\ I^{t2}_{cM}(\zeta,\tau) &= I_{s,z0}(\tau) \cdot \alpha_{cM}(\zeta,\tau) \\ I_{s,z0}(\tau) &= \gamma_{z0}(\tau) I^i_{bM}(z_0,\tau) \end{aligned} \tag{9}$$

Both (8) and (9) indicate that currents propagate with the attenuation coefficient α_{xM} in a stage from a (virtual) source,

just like the wave prorogation in an infinitely-long dipole line model shown in Section III.

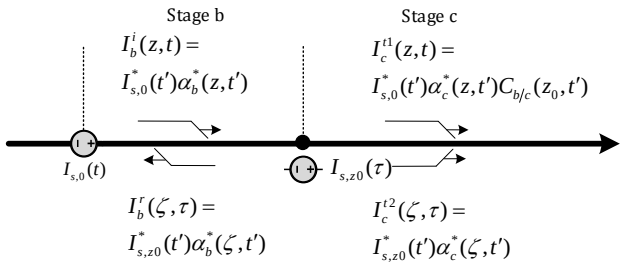

Fig. 4 Traveling wave theory for the dipole line model with a discontinuity

Now introduce coefficients $\alpha_x^*(z,t')$ and $\gamma_{zs}^*(z,t')$ expressed with time t', given by a source at $z = zs$. t' is the time counting after the wave arrives at point z, for example, $\alpha_x^*(z,t') = \alpha_x(z,t)|_{t=t'+\Delta t}$, where Δt is the travel time of a wave from the source point (zs) to the field point (z). Both (8) and (9) then are revised to be

$$\begin{aligned} I_b^i(z,t) &= I_{s,0}^*(t')\cdot\alpha_b^*(z,t') \\ I_c^{t1}(z,t) &= I_{s,0}^*(t')\cdot\alpha_c^*(z,t')\cdot C_{b/c}^*(z_0,t') \\ I_b^r(\zeta,\tau) &= I_{s,z0}^*(t')\cdot\alpha_b^*(\zeta,t') \\ I_c^{t2}(\zeta,\tau) &= I_{s,z0}^*(t')\cdot\alpha_c^*(\zeta,t') \end{aligned} \tag{10}$$

where correction factor $C_{b/c}^*(z_0,t')$ is defined as $\alpha_b^*(z_0,t')/\alpha_c^*(z_0,t')$, arising at the discontinuity (z_0) for the source at $z = 0$. All the currents in wires b and c in (10) are expressed with local time t' accounting after the wave arrives at field point z.

In [3] a lattice mesh was employed to describe the wave propagation on the line consisting of a set of equally time-spaced segments. The generalized Lattice element was presented to illustrate the relationship among different wave components. By adopting this approach, wave propagation over a line discontinuity in the multi-dipole model can then be described graphically. Fig. 4 depicts the traveling wave theory for wave propagation on the dipole line model. The incident current I^i travels with attenuation towards the discontinuity. After the discontinuity, it continues to propagate as $I^{t1}$with a new attenuation coefficient multiplied by a correction factor. This wave is called the primary wave. A pair of secondary waves I^r and I^{t2} are generated at the discontinuity. This case is similar to a delta-gap dipole fed with the incident current $I_{s,z0}$. Note that both the reflection coefficient and attenuation coefficient are time-variant and are affected by source position. The generalized Lattice element in [3] cannot be applied directly in this case.

V. Simulation The Response of the Source Current or Voltage with an Arbitrary Waveform

In the previous sections, the dipole is fed by a delta-gap voltage source with a ramp feed current. To find out the dipole response under an arbitrary-waveform current, a convolution technique is adopted. Assume that the dipole response under a ramp feed current is $e_i(t)$, which is obtained with the traveling wave theory. According to the convolution properties in a linear time-invariant system [32], the impulse response $h_i(t)$ of the dipole is derived to be

$$h_i(t) = \frac{d^2 e_i(t)}{dt^2} \tag{11}$$

Then, response $y(t)$ of the dipole under an arbitrary-waveform feed current $I_s(t)$ is written as:

$$y(t) = I_s(t) * h_i(t) \tag{12}$$

Note that the response of the current given by the step delta-gap voltage is presented in [27]

$$I_{step}(z,t) = \frac{u(t-z/c)}{\sqrt{\mu_0/\varepsilon_0}} \tan^{-1}\left(\frac{\pi}{2\ln\sqrt{c^2t^2-z^2}/r}\right) \tag{13}$$

Then, the impulse response $h_v(z,t)$ of feed-point current in the dipole excited by a step voltage source can be expressed by the step response $I_{step}(z,t)$ [32], as follows:

$$\begin{aligned} h_0(t) &= dI_{step}(0,t)/dt \\ &= \sqrt{\frac{\varepsilon_0}{\mu_0}}\left[\delta(t)\tan^{-1}\left(\frac{\pi/2}{\ln(ct/r)}\right) - \frac{u(t)}{\pi t\ln(ct/r)+4}\right] \end{aligned} \tag{14}$$

The dipole response $y(t)$ under the source voltage $V_s(t)$ then is expressed by

$$y(t) = [V_s(t) * h_0(t)] * h_i(t) \tag{15}$$

The evaluation of the dipole response is illustrated in Fig. 5.

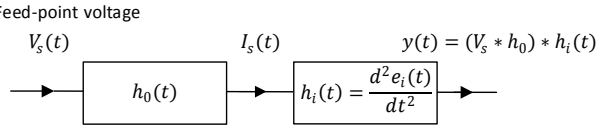

Fig. 5 Flowchart of dipole response evaluation given by the source voltage

VI. Simulation Result and Comparison of Waves in a Tower Structure

A. Numerical Comparison with FDTD

Lightning transient currents in a two-stage tower on the ground, as shown in Fig. 1, are simulated with the proposed approach. The tower is 240 m tall with 120 m height in each stage. The conductors have radii of 0.01 m and 0.03 m and wire spacing of 2.4 m and 4.8 m, respectively, in the upper and lower stages. The tower is connected to a grounding electrode with a resistance of 10 Ohm, simulating the effect of the lossy ground. It is found in [23,35] that the lossy ground behaves like a perfect ground to the tower conductors above ground. Therefore, the lossy ground is treated as a perfect ground, and is substituted with the tower image connected to the grounding resistance, as shown in Fig. 6.

The tower is struck by lightning at its tip. The lightning channel above the tower is represented by a vertical wire with a radius of 0.01m. The incident current $I_{s,0}(t)$ resulting from a lightning return stroke that has a magnitude of 10 kA and a waveform of 0.25/100 μs. It is expressed using the Heidler's function [29]. In the simulation, the traveling wave theory is first employed to calculate the transient current $I_r(t)$ with a

ramp incident current. Lightning current $I_p(t)$ at point p given by incident current $I_{s,0}(t)$ then is calculated using a convolution technique presented in section V, as follows:

$$I_p(t) = \frac{d^2 I_{s,0}(t)}{dt^2} * I_r(t) \tag{16}$$

As shown in Fig. 6, incident current I^i as a primary wave propagates with attenuation towards the other end of the model. The wave is reflected with γ_0^* at $z = 0$ or $2H$. The subsequent propagation in the model can be viewed as a new primary wave arising from a brand-new source at $z = 0$ or $2H$. Fig. 7(a) shows a lattice diagram for the primary waves propagating along the model, which originate at one end of the model. The total attenuation for a wave propagating from one end towards another after three discontinuities including the reflection at one end is expressed by

$$K(z,t') = \gamma_0^*(t')\alpha_b^*(z,t')C_{b/c}^*(z_0,t')C_{b/c}^*(3z_0,t') \tag{17}$$

where t' is the time counting after the wave reaches point z.

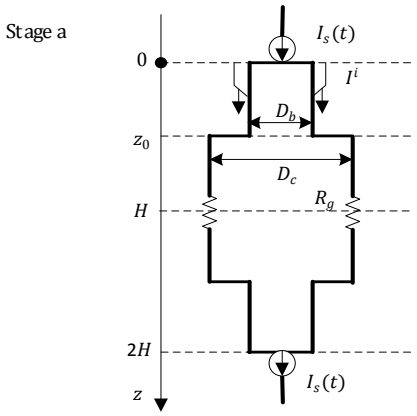

Fig.6 Tower model struck by lightning (z_0 = 120 m and H = $2z_0$; r_a = 0.001 m, r_b = 0.01 m and r_c = 0.03 m; D_a = 2.4 m and D_b = 4.8 m)

Consider a primary wave arriving at point z in stage b in the *nth* one-way trip in the model. The primary wave $I_{pri}^{(n)}$ can be expressed with (10) and (17) as

$$I_{pri}^{(n)}(z,t') = \begin{cases} I_{s,0}^*(t')\alpha_b^*(z,t')\cdot K^{n-1}(2H,t') & n = 2i \\ I_{s,0}^*(t')K(2H-z,t')\cdot K^{n-1}(2H,t') & n = 2i+1 \end{cases} \tag{18}$$

where $i = 0,1\cdots$. $K(2H,t')$ is the totoal attenuation of current on a one-way trip including the reflection at one end. Both $\alpha_b^*(z,t')$ and $K(2H-z,t')$ are respectively the attenuations from two ends to point z on a one-way trip.

The primary wave will generate a virtual source at each of discontinuities $(z = 0,\ z_0,\ H,\ z_0 + H, 2H)$, which is determined by the reflection coefficient there. Fig. 8 shows the reflection coefficients of a current wave between stages b and c, and at the tower tip calculated with (7a). It is found that the reflection coefficients change dramatically at an early time, but tend to be constant after 0.2 μs.

At each discontinuity, the virtual source generates a pair of secondary waves propagating in two opposite directions. Similar to the primary wave, these secondary waves will produce a next-level virtual source at each discontinuity they encounter. As the reflection coefficients are generally less than 0.1, as seen in Fig. 8, the next-level secondary waves could be neglected. The two secondary waves arriving at point z in stage b after the (n-1)*th* full reflection, arising from the 1st virtual current source $z = z_0$, is expressed by

$$I_{\text{sec},1a}^{(n)}(z,t') = I_{s,z0}^*(t')\alpha_b^*(z_0,t')\cdot \begin{cases} \alpha_b^*(z,t')/\alpha_b^*(z_0,t') & n = 0 \\ \alpha_b^*(z,t')K^n(2H,t') & n = 2i+1 \\ K(2H-z,t')K^n(2H,t') & n = 2i+2 \end{cases} \tag{19}$$

$$I_{\text{sec},1b}^{(n)}(z,t') = I_{s,z0}^*(t')\alpha_b^*(3z_0,t')C_{c/b}(2z_0,t') \begin{cases} K(2H-z,t')K^n(2H,t') & n = 2i+1 \\ \alpha_b^*(z,t')K^n(2H,t') & n = 2i+2 \end{cases} \tag{20}$$

where $i = 0,1\cdots$. Fig. 7(b) shows a lattice diagram for the propagation of a pair of the secondary waves arising from a virtual source at $z = z_0$.

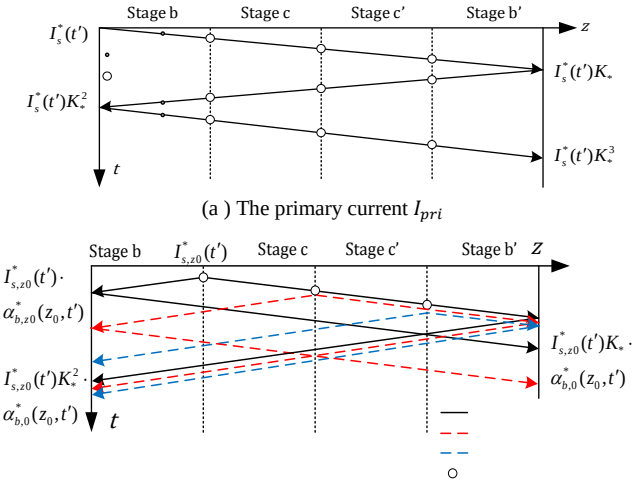

(a) The primary current I_{pri}

(b) The level 1 secondary waves generated by the primary wave (currents presented in the diagram are for the 1st sec. wave only)

Fig.7 Illustration of traveling waves in a 2-stage tower, $K_* = K(2H,\tau')$

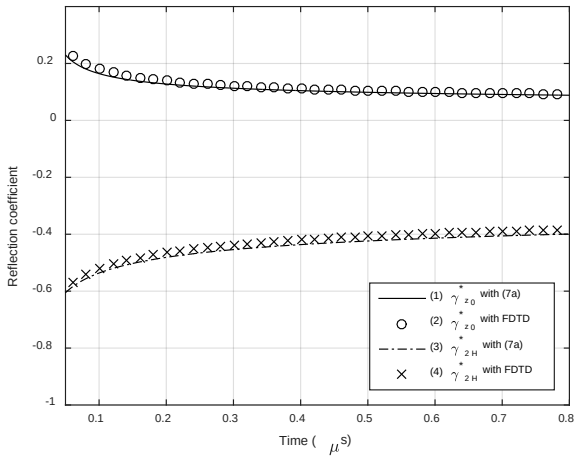

Fig.8 Reflection coefficient γ_{z0}^* between stages b and c and γ_{2H}^* at the tower tip calculated by the proposed method and FDTD method.

The tower current is simulated with the proposed method when the tower tip is struck by lightning. Fig. 9(a) illustrates both the primary and secondary waves arriving at $z = 50\ m$ up to the 3rd one-way trip on the structure. It is found that the 1st-level secondary waves are relatively small due to the small reflection coefficient. Their subsequent secondary waves can, therefore, be ignored. Fig. 9(b) shows the curve of the resultant current at the observation point calculated using the traveling wave theory.

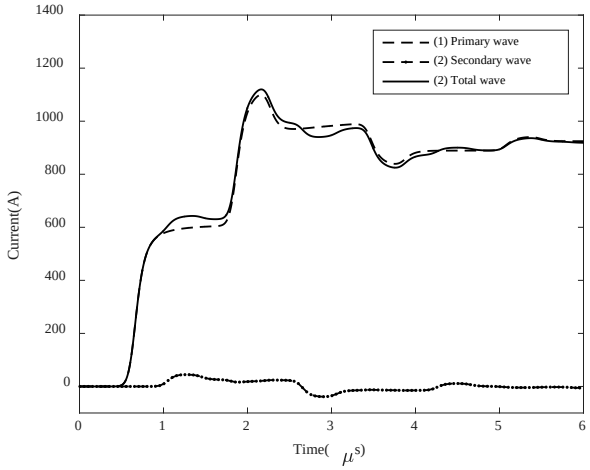

(a)

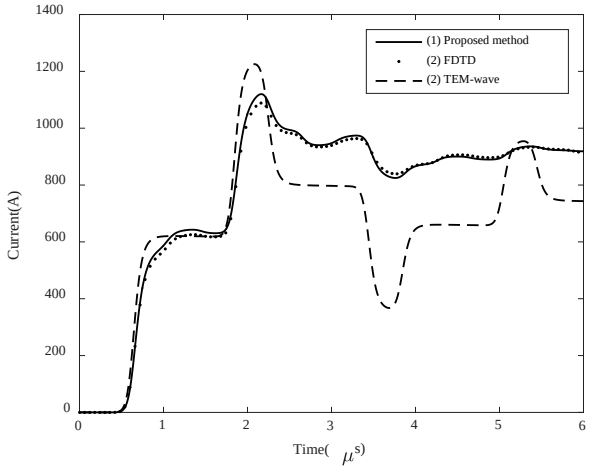

(b)

Fig.9 Comparison of tower currents calculated with the extended traveling wave theory, the FDTD method and the traditional TL model

Both reflection coefficients and the total current in the tower also are calculated by the FDTD method for comparison. In the FDTD simulation, the working space consists of 200, 200 and 500 FDTD steps in the x, y and z directions, respectively. A non-uniform mesh technique is adopted in the horizontal direction. The cell size near the tower is selected to be 0.6 m, and is increased to 54m gradually. A PEC layer covers the bottom boundary of the working space, and PML ABC layers cover the other boundaries. The conductors of the tower in the FDTD simulation are represented with the thin-wire model [30-31]. The lead wire is represented with the thin-wire mode as well, and is extended from the tower vertically to the absorbing boundary of the working domain. This arrangement mimics a semi-infinitely long wire for the lightning channel. The time step in the simulation is set to be 1 ns.

The reflection coefficients calculated by the FDTD method are presented in Fig. 8. It is found that the results calculated by two methods generally match well. The difference is less than 2% in the middle of the tower, and 5% at the tower tip. This difference may be introduced by neglecting the wave propagation effect along horizontal conductors. The resultant current calculated with the FDTD method is presented in Fig. 9(b). It is found that both curves match very well with a difference of 2%. The TEM solution based on the traditional TL is also calculated for comparison. The reflection coefficient at the tower tip is assumed to be -0.7 and at the other discontinuities is zero. A significant difference between the traditional TL theory and the proposed traveling theory is observed.

B. Experimental Comparison

The measurement result for a tower under a lightning strikes with a vertical lead wire was presented in [36].

Tower	Scale
a	0.668
b	0.802
c	1.364
d	0.928
e	0.334
f	0.615
g	0.535
h	1.516
i	0.49
Height	3

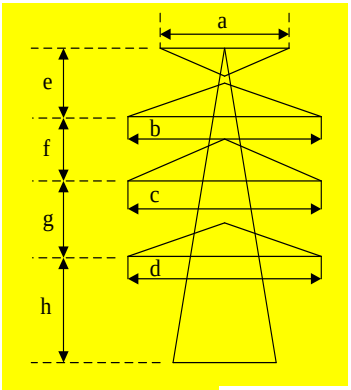

a) Original configuration

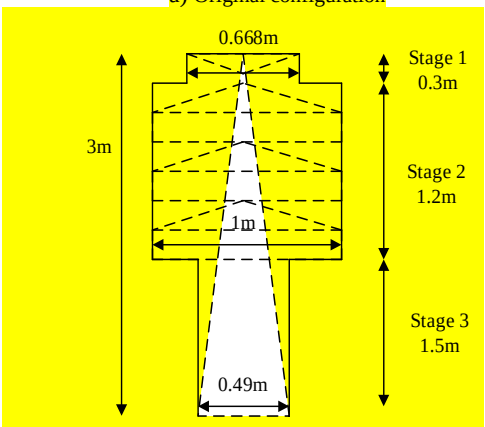

(b) Simplified 3-stage configuration for simulation

Fig. 10 The configuration for experimental validation

Fig.10a shows the original configuration of the tower. Fig.10b shows the modified configuration by neglecting the horizontal wires for the simulation using the proposed method. The tower is represented by a three-stage structure with a horizontal wire spacing of 0.24 m in the top stage and 0.49 m in the bottom stage. Stages 1, 2 nd 3 have the heights of 0.3

m, 1.2 m and 1.5 m, and the widths of 0.668 m, 1 m [(b+c+d)/3=1 m] and 0.49 m, respectively. Both Stages 1 and 2 have 8 legs (4 for brace arms and 4 for tower legs), and Stage 3 has 4 legs only. The tower is connected to a grounding resistance of 30 Ohm, according to [36].

Fig. 11 shows the simulated step response obtained with the proposed method together with the measured result given in [36] for comparison. It is found, in the simulated response waveform, the clear wave reflections arising at joints between Stages 1 and 2, Stages 2 and 3, and at the ground. Because of these wave reflections, the waveform changes its slope, and matchs with the measured waveform well. The minor discrepancies between these two waveforms may be caused by replacing those horizontal arms with a set of vertical wires in Stages 1 and 2.

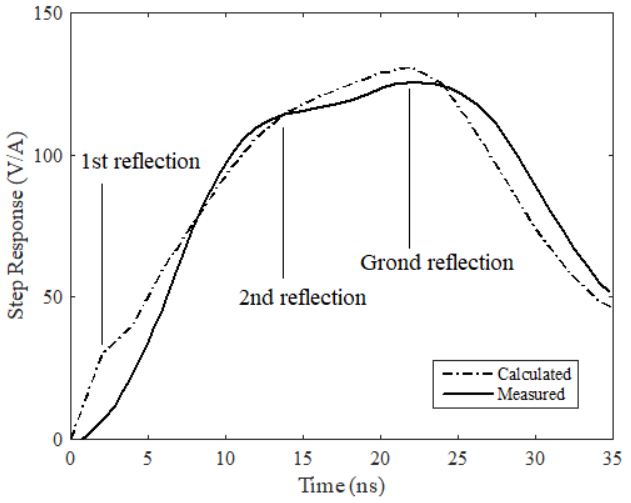

Fig.11 comparison for measured and simulated results in a tower [36]

VII. CONCLUSIONS

This paper presented a theoretical time-domain analysis of lightning transients in a vertical tower. The multiple-stage tower was represented with a model of multi-dipole lines with a discontinuity. A time-domain traveling wave theory was introduced to depict the non-TEM wave propagation on such a tower. The attenuated propagation of current waves in the tower is formulated. Analytical formulas are provided for time/position-variant characteristic impedance of the line at any position and any time, as well as the time-variant reflection coefficient at each discontinuity.

In the traveling wave theory, both the primary waves and secondary waves are proposed to depict a complicated multiple reflection situation. The primary wave is the incident current wave attenuating in its propagation along the tower and is corrected with a factor when crossing over a discontinuity. A pair of secondary waves are generated at the discontinuity. All these waves are characterized by the unique transient impedance of a multi-dipole line model.

The proposed time-domain traveling wave theory has been applied to evaluate lightning currents in a two-stage tower. It is found that the secondary waves could be neglected if the reflection coefficient at a discontinuity is small. This proposed method has been compared with the FDTD method and TL theory. A good agreement with the FDTD method is observed. A significant error is found if the traditional TL model is used. A comparsion with the experiment result reported in the literature is made, and a good agreement is observed.

ACKNOWLEDGMENTS

The work leading to this paper was supported by grants from the Research Grants Council of the HKSAR (Project No. 15208019 and 15210018).

REFERENCE

[1] T. Hara and O. Yamamoto, "Modelling of a transmission tower for lightning-surge analysis," IEE Proc.-Gener. Transm. Distrib., vol. 143 no.3, 1996, pp. 283-289.

[2] T.Yamada, A. Mochizuki, J. Sawada, E. Zaima, T. Kawamura, A. Ametani and S. Kato. "Experimental evaluation of a UHV tower model for lightning surge analysis." IEEE Trans on PWRD, vol. 10 no.1, 1995, pp. 393-402.

[3] W. A. Chisholm, Y. L. Chow and K. D. Srivastava. "Lighting Surge response of transmission towers." IEEE Trans. on PAS vol. 9, 1983, pp. 3232-3242.

[4] J. A. Martinez and F. Castro-Aranda. "Tower modeling for lightning analysis of overhead transmission lines." IEEE Power Engineering Society General Meeting, 2005

[5] F. Rachidi, W. Janischewskyj, A. M. Hussein, C. A. Nucci, S. Guerrieri, B. Kordi and J. S. Chang. "Current and electromagnetic field associated with lightning-return strokes to tall towers." IEEE Trans. on EMC, vol. 43 no.3, 2001, pp. 356-367.

[6] B. Kordi, R. Moini, W. Janischewskyj, A. M. Hussein, V. O. Shostak and V. A. Rakov. "Application of the antenna theory model to a tall tower struck by lightning." JGR: Atmospheres, 108.D17, 2003, 4542

[7] C.F. Wagner and A.R. Hileman, "A new approach to the calculation of the lightning performance of transmission lines – Part III," AIEEE Trans. Part III, vol. 79, no. 3, 1960, pp. 589-603

[8] M.A. Sargent and M. Darveniza, "Tower surge impedance," IEEE Trans. on PAS, vol. 88, no. 3, 1969, pp. 680-687

[9] W.A. Chisholm, Y.L. Chow and K.D. Srivastava, "Travel time of transmission towers," IEEE Trans. on PAS, vol. 104, no. 10, 1985, pp. 2922-2928

[10] A. Ametani et al., "Frequency-dependent impedance of vertical conductors and a multiconductor tower model," IEE Proc.-Gener. Transm. Distrib., vol. 141, no. 4, July 1994, pp. 339-345

[11] T. Hara and O. Yamamoto, "Modelling of a transmission tower for lightning surge analysis," IEE Proc.-Gener. Transm. Distrib., vol. 143, no. 3, 1996, pp. 283-289

[12] J.A. Gutierrez et al., "Nonuniform transmission tower model for lightning transient studies," IEEE Trans. on PWRD, vol. 19, no. 2, pp. 490-496, April 2004.

[13] Y. Baba and M. Ishii, "Numerical electromagnetic field analysis on lightning surge response of tower with shield wire," IEEE Trans. On PWRD, vol. 15, no. 3, pp. 1010-1015, July 2000.

[14] T. Ito et al., "Lightning flashover on 77-kV systems: Observed voltage bias effects and analysis," IEEE Trans. on PWRD, vol. 18, no. 2, pp. 545-550, April 2003.

[15] D. Pavanello, F. Rachidi, W. Janischewskyj, M. Rubinstein, A. M. Hussein, E. Petrache, V. Shostak, I. Boev, C. A. Nucci, W. A. Chisholm, M. Nyffeler, J. S. Chang and A. Jaquier. "On return stroke currents and remote electromagnetic fields associated with lightning strikes to tall structures: 1. Computational models." *Journal of Geophysical Research: Atmospheres*, vol. 112, D13122, 2007,

[16] F. Rachidi, V. A. Rakov, C. A. Nucci and J. L. Bermudez. "Effect of vertically extended strike object on the distribution of current along the

lightning channel." *Journal of Geophysical Research: Atmospheres*, vol. 107, D23, 4699, 2002.
[17] J. L. Bermudez, M. Rubinstein, F. Rachidi, F. Heidler and M. Paolone. "Determination of reflection coefficients at the top and bottom of elevated strike objects struck by lightning." *Journal of Geophysical Research: Atmospheres*, vol. 108, D14, 4413, 2003.
[18] Y. Baba And V. A. Rakov, "On The Mechanism of Attenuation of Current Waves Propagating Along a Vertical Perfectly Conducting Wire Above Ground: Application To Lightning," IEEE Trans. on EMC, Vol. 47, No. 3, pp. 521–532, Aug. 2005.
[19] L. Grcev, and R. Farhad. "On tower impedances for transient analysis." IEEE Trans. on PWRD, vol. 19 no.3, 2004, pp. 1238-1244.
[20] R. Lundholm, R. B. Finn, and W. S. Price, "Calculation of transmission line lightning voltages by field concepts," Trans. Amer. Inst. Electr. Eng. Part III, Power App. Syst., vol. 76, pp. 1271–1281, 1957.
[21] A. Shoory, F. Vega, P. Yutthagowith, F. Rachidi, Rubinstein, Y. Baba and A. Ametani., "On the mechanism of current pulse propagation along conical structures: Application to tall towers struck by lightning," IEEE Trans. EMC, vol. 54, no. 2, pp. 332–342, Apr. 2012.
[22] J. Takami, T. Tsuboi, and S. Okabe, "Measured distortion of current waves and electrical potentials with propagation of a spherical surge in an electromagnetic field," IEEE Trans. on EMC, vol. 52, no. 3, pp. 753–756, Aug. 2010.
[23] Y. Ding, Y. Du, and M. Chen. "Lightning surge propagation on a grounded vertical conductor." IEEE Trans. on EMC, vol. 60 no.1, 2017, pp. 276-279.
[24] Y. Du, X. Wang, And M. Chen, "Numerical Investigation Of Transient Surge Impedance Of A Vertical Conductor Over A Perfect Ground," Electric Power Syst. Res., Vol. 94, pp. 106–112, 2013.
[25] X. Wang, Y. Du, M. Chen, and X. Huang, "Surge Behavior At The Discontinuity Of A Vertical Line Over The Ground," Electric Power Syst. Res., Vol. 113, pp. 129–133, 2014.
[26] Y. Du and Y. Ding. "Lightning surge propagation on a single conductor in free space." IEEE Trans. on EMC, vol. 59 no.1, 2016, pp. 19-127.
[27] J. D. Kraus and K. R. Carver "Electromagnetics", p485-489, second edition, 1984.
[28] K. C. Chen, "Transient response of an infinite cylindrical antenna," IEEE Trans. AP., Vol. 31, No. 1, pp. 170–172, Jan. 1983.
[29] F. Heidler, "Traveling current source model for LEMP calculation," Proc. of the 6th Int. Zurich Symp. EMC, Zurich, Switzerland, 1985, pp.157~162.
[30] Y. Du, B. Li and M. Chen, "The Extended Thin-Wire Model of Lossy Round Wire Structures for FDTD Simulations," in IEEE Trans. on PWRD, vol. 32, no. 6, pp. 2472-2480, Dec. 2017.
[31] B. Li, Y. Du and M. Chen, "Thin-wire Models for Inclined Conductors with Frequency-dependent Losses," IEEE Trans on PWRD, vol. 35 no. 3, 2020, pp. 1083-1092
[32] S. Tkatchenko, R. Farhad, and I. Michel. "Electromagnetic field coupling to a line of finite length: Theory and fast iterative solutions in frequency and time domains." IEEE Trans. on EMC , vol. 37 no.4, 1995, pp. 509-518.
[33] Bogerd, Johan C., Anton G. Tijhuis, and J. J. A. Klaasen. "Electromagnetic excitation of a thin wire: A traveling-wave approach." IEEE Trans. on AP, vol. 46 no.8, 1998, pp. 1202-1211.
[34] K. Okumura and J. Kijima, "A method for computing surge impedance of transmission tower by electromagnetic field theory", IEEJ Trans. Power & Energy, vol. B-105, no. 9, pp. 733-740, 1985 (in Japanese).
[35] Y. Du, X. Wang and M. Chen. "Circuit parameters of vertical wires above a lossy ground in PEEC models." IEEE transaction on EMC 54.4 (2011): 871-879.
[36] H. Motoyama and H. Matsubara, "Analytical and experimental study on surge response of transmission tower," IEEE Trans. Power Delivery., vol.15, no.2, pp. 812-819, April 2000.
[37] K. Chen, "Transient response of an infinite cylindrical antenna." IEEE Trans on AP vol.31, no.1, 1983, pp. 170-172
[38] Y.Dong, Y.Du, and M.chen. "Surges on a vertical conductor excited by current and voltage sources." The 10th Asia-Pacific International Conference on Lightning, Krabi, Thailand, 16-19 May 2017.

Appendix A Lossless Propgation of Potnetials

Note that the longitudinal E field is zero on a perfect conductor. In the n-dipole line model given in Fig. 1(a), both vector potential A_{xM} and scalar potential ϕ_{xM} ($x = a, b$ or b) on the line satisfy the following eqaution,

$$\partial\phi_{xM}(z,t)/\partial z = -\partial A_{xM}(z,t)/\partial t \tag{A1}$$

With Lorenz gauge, the following is obtained,

$$\begin{aligned}\partial\phi_{xM}(z,t)/\partial t &= -c^2\nabla\cdot A_{xM}(z,t)\\ &= -c^2\,\partial A_{xM}(z,t)/\partial z\end{aligned} \tag{A2}$$

Note that (A1) and (A2) formulate a pair of coupled 1st order differential equations similar to the well-known telegrapher's equations. Then, the corresponding solution for the vector potential is given by [27]:

$$A_{xM}(z,t) = f_1(ct-z) + f_2(ct+z) \tag{A3}$$

Under the zero initial condition, integrating (A3) along the time axis yields

$$\begin{aligned}\phi_{xM}(z,t) &= -c^2\int_0^t \partial A_{xM}(z,t)/\partial z dt\\ &= c^2\int_0^t [\partial f_1/c\partial t - \partial f_2/c\partial t]\,dt\\ &= cf_1(ct-z) - cf_2(ct+z)\end{aligned} \tag{A4}$$

Thus, for a wave propagating in one direction, these vector potential and scalar potential satisfies:

$$\phi_{xM}(z,t) = \pm cA_{xM}(z,t) \tag{A5}$$

where the " + " sign is taken for the a wave propagating in the positive direction, and the "– " sign in the negative direction.

Appendix B Wave Propagation in a Multiple Dipole Line Structure

To obtain characteristic equations for waves in a multiple dipole line structure shown in Fig. 2(a), the current in dipole line 1 is decomposed into two components, ie., $-(n-1)I_{b1}$ and nI_{b1} as seen in Fig. 2(b) and (c). Therefore, there are n pairs of dipole lines or n transmission lines with dipole line 1 being the reference, as illustrated in Fig. 2(b). Each pair of the dipole lines carries two equal but opposite currents. In Fig. 2(c), there is one dipole line alone carrying the current of nI_{b1}. Note that all these currents are characterized by the same attenuation coefficient $\alpha_{bM}(z,t)$.

Now consider a pair of dipole lines 1 and i with spacing $D_{b,1i}$, as shown in Fig.2(b). These dipole lines are closely spaced and carry equal but opposite currents. Assume that $A'_{bi}(r,z,t)$ is the vector potential contributed by the current in line i. Note that $A'_{b1}(D_{b,1i},z,t) = A'_{bi}(r_b,z,t)$. With Ampere's law, the vector potential resulting from a pair of dipole lines with the opposite currents is given by

$$A'_{b1}(r_b,z,t)-A'_{b1}(D_{b,1i},z,t)=\int_{r_b}^{D_{b,1i}}B(r,z,t)dr \approx \frac{\mu_0}{2\pi n}\ln\left(\frac{D_{b,1i}}{r_b}\right)I_{bM}(z,t) \quad \text{(B1)}$$

where $I_{bM}=nI_{b1}$. Vector potential A''_{b1} in Fig. 2(c) is contributed by the current on a single dipole line with the radius r_b. According to [26], it is expressed by

$$A''_{b1}(z,t)=\frac{\mu_0}{4\pi}\int_{(z-ct)/2}^{(z+ct)/2}\frac{I_{bM}(|l'|,t_{d1})}{\sqrt{(l'-z)^2+r_b^2}}dl' \quad \text{(B2)}$$

where $t_{d1}=t-|l'-z|/c$.

Note that the current can be written, using the attenuation coefficient, as $I_{bM}(|l'|,t_{d1})=I_s(0,t_{d2})\alpha_{bM}(|l'|,t_{d1})$ [26]. Then, the total vector potential A_{bM} on an n-dipole line structure in Fig. 2(a) is obtained by summing both (B1) and (B2), as follows:

$$A_{bM}(z,t)=A'_{b1}(z,t)+A''_{b1}(z,t) =\frac{\mu_0}{4\pi}\int_{(z-ct)/2}^{(z+ct)/2}\frac{I_{s,0}(t_{d1})\alpha_{bM}(|l'|,t_{d1})}{\sqrt{(l'-z)^2+r_b^2}}dl'- I_{bM}(z,t)\frac{\mu_0}{2\pi n}\sum_{i=1}^{n}\ln(\frac{D_{1i}}{r_b}) \quad \text{(B3)}$$

Now we replace $\alpha_{bM}(|l'|,t_{d1})$ in the integral of (B3) with $\alpha_{bM}(z,t)+[\alpha_{bM}(|l'|,t_{d1})-\alpha_{bM}(z,t)]$. According to the Bogerd's derivation for a finite antenna [33], the integral containing $[\alpha_{bM}(|l'|,t_{d1})-\alpha_{bM}(z,t)]$ is neglected. The remaining integral can be evaluated analytically under the assumption that $(ct-z)^2 \gg r^2$. Thus, the final expression for the total vector potential in (B3) is given as,

$$A_{bM}(z,t)= I_{bM}(z,t)\frac{\mu_0}{2\pi n}\sum_{i=1}^{n}\ln(\frac{D_{1i}}{r_b})+I_{bM}(z,t)\cdot \frac{\mu_0}{2\pi}\left(\frac{z}{ct-z}\ln\frac{ct+z}{\sqrt{z^2+r^2}+z}+\ln\frac{\sqrt{c^2t^2-z^2}}{r}-1\right) \quad \text{(B4)}$$

Thus, the analytical expression for transient impedance can be obtained as

$$Z_{bM}(z,t)=\frac{\phi_{bM}(z,t)}{I_{bM}(z,t)}=\frac{cA_{bM}(z,t)}{I_{bM}(z,t)} =Z_b(z,t)-\frac{\mu_0 c}{2\pi n}\sum_{i=1}^{n}\ln(\frac{D_{1i}}{r_b}) \quad \text{(B5)}$$

and

$$Z_b(z,t)=\frac{\mu_0 c}{2\pi}\left(\frac{z}{ct-z}\ln\frac{ct+z}{\sqrt{z^2+r^2}+z}+\ln\frac{\sqrt{c^2t^2-z^2}}{r}-1\right) \quad \text{(B6)}$$

It is found that under the thin-wire approximation, the transient impedance of a multi-dipole line structure is not affected by the attenuation coefficient α_{bM} of current. It is fully determined by the geometry of a wire structure. This impedance can be viewed as the impedance of a standalone dipole minus a quasi-static transmission line impedance.

An alternative expression of standalone dipole impedance under a step-function voltage source is presented by K. Chan in [37] and discussed by Y. baba in [18]. By using the proposed convolution in Section V, the ramp response current $I_{ramp}(z,t)$ in the dipole can be obtained as follows

$$I_{ramp}(z,t)=r(t)*h_0(z,t) =r(t)*\frac{dI_{step}(z,t)}{dt}=\frac{dr(t)}{dt}*I_{step}(z,t) =\int_{z/c}^{t}I_{step}(z,t')dt' \quad \text{(B7)}$$

where $r(t)$ is the ramp waveform and $I_{step}(z,t)$ defined in (13). Note that potential $\phi(t)$ in this paper is defined with reference to infinity. As the dipole structure is symmetrical, $\phi(t)$ is half of the gap voltage $u(t)$. Then the transient impedance of the dipole fed by a ramp source voltage is derived to be

$$Z(z,t)=\frac{\phi_{ramp}(z,t)}{I_{ramp}(z,t)}=\frac{\int_{z/c}^{t}u(t'-z/c)dt'}{2\int_{z/c}^{t}I_{step}(z,t')dt'} \quad \text{(B8)}$$

It is known in [38] that the transient impedances of a dipole, fed by a ramp source current source and a ramp source voltage, are almost the same. Therefore, (B8) can be also applied to calculate the transient impedance of the dipole under a ramp-wave source current.

Both (B6) and (B8) can be applied to evaluate the impedance of a standalone dipole. The former one is based on Bogerd's derivation and the later one is based on K. Chan's derivation.

APPENDIX C TRANSIENT IMPEDANCE OF WAVE PROPAGATION IN A MULTI-STAGE TOWER

Consider an n-dipole line structure with a change of wire spacing at $z=z_0$, as illustrated in Fig. C1(a). With the same technique used in Appendix B, the current in dipole line 1 is substituted by $-(n-1)I_{x1}$ and nI_{x1} in Fig. C1(b) and nI_{x1} in Fig. C1(c) ($x=a,b$ or $,c$).

Similar to (B1) in Appendix B, vector potential in Stage x contributed by a pair of opposite currents shown in Fig. C1(b) is expressed by

$$A_{DM}(r_x,z,t)=\int_{r_x}^{D_{x,1i}}B(r,z,t)dr =\frac{\mu_0}{2\pi n}\ln\left(\frac{D_{x,1i}}{r_x}\right)I_{x1}(z,t) \quad \text{(C1)}$$

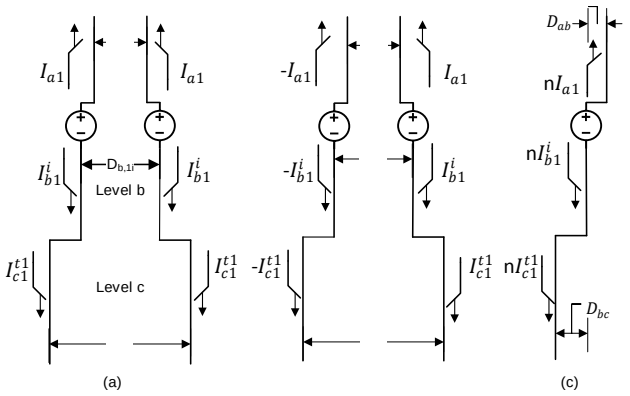

Fig. C1 Waves propagating in a multiple dipole line structure (a) original configuration (b) *n* pairs of dipole lines (c) a single dipole line

Similar to (B2), the vector potential A''_{x1} on a single dipole line with the radius r_x shown in Fig. 2(c) is given by:

$$A''_{xM}(z,t)=\frac{\mu_0 c}{4\pi}\int_{(z-ct)/2}^{(z+ct)/2}\frac{I_{xM}(|l'|,t_{d1})}{\sqrt{\Delta l'^2+r_x^{\,2}}}dl'+\frac{\mu_0 c}{4\pi}\int_{(z-ct)/2}^{(z+ct)/2}\frac{I_{yM}(|l'|,t_{d2})}{\sqrt{\Delta l'^2+D_{xy}^{\,2}}}dl' \tag{C2}$$

where y represents a stage other than stage x. D_{xy} is equal to $(D_{y,ij}-D_{x,ij})/2$. The total current is composed up by I_{xM} and I_{yM}, where $I_{xM}=0$ outside the stage x and $I_{yM}=0$ at stage x.

Note that (C2) can also be written as:

$$A''_{xM}(z,t)=\frac{\mu_0 c}{4\pi}\int_{(z-ct)/2}^{(z+ct)/2}\frac{I_{xM}(|l'|,t_{d1})+I_{yM}(|l'|,t_{d2})}{\sqrt{\Delta l'^2+r_x^{\,2}}}dl'-\frac{\mu_0 c}{4\pi}\int_{(z-ct)/2}^{(z+ct)/2}\frac{I_{yM}(|l'|,t_{d1})}{\sqrt{\Delta l'^2+r_x^{\,2}}}-\frac{I_{yM}(|l'|,t_{d2})}{\sqrt{\Delta l'^2+D_{xy}^{\,2}}}dl' \tag{C3}$$

Where, $t_{d2}=t-\sqrt{\Delta l'^2+D_{xy}^2}\,/c$ is the retardation time over the spacing distance of dipole lines.

The second term in the right-hand side of (C3) can be viewed as the differential-mode vector potential $A'_{x1}(D_{xy},z,t)-A'_{x1}(r_x,z,t)$ contributed by the current I_{yM} on a single dipole line. Similar as the derivation in appendix B, this vector potential difference can be evaluated by the integral of magnetic flux. Then, by approximated with the Ampere's circuit law that $\mu_0 I=\oint B\,dl=2\pi rB$ for a single line,

$$A'_{x1}(r_x,z,t)-A'_{x1}(D_{xy},z,t)=\int_{r_x}^{D_{xy}}B(r,z,t)dr\approx\frac{\mu_0}{2\pi n}\ln\left(\frac{D_{xy}}{r_x}\right)I_{yM}(z,t) \tag{C4}$$

As mentioned before, the observation point is at stage x, where $I_{yM}=0$. Thus, (C4) is always zero. This means the second term in the right-hand side of (C3) can be removed. It is noted that the approximation in (C4) is based on the Ampere's circuit law, this yields a quasi-static approximation on the differential-mode vector potential for a closely spaced dipole lines.

The total vector potential can then be obtained by summing both (C1) and (C3). The total transient impedance of the *n*-dipole line structure in stage x is obtained as follows:

$$Z_{xM}(z,t)=\frac{cA_{xM}(z,t)}{I_{xM}(z,t)}=Z_x(z,t)-\frac{\mu_0 c}{2\pi n}\sum_{i=1}^{n}\ln\left(\frac{D_{1i}}{r_x}\right) \tag{C5}$$

where $Z_x(z,t)$ can be calculated with (B6) or (B8). The transient impedance in stage x of the tower with a discontinuity is determined by the single dipole line impedance together with the quasi-static transmission line impedance. Note that (C5) is the same as (B5).